

## Use of chemically activated termite feces a low-cost adsorbent for the adsorption of norfloxacin from aqueous solution

Tamiris Chahm, Larissa Fátima de Souza, Nathalia Ramos dos Santos, Bruna Aparecida da Silva and Clovis Antonio Rodrigues

### ABSTRACT

Antibiotics, as emerging contaminants, are of global concern due to the development of antibiotic resistant microorganisms. Current wastewater treatment technology cannot efficiently remove sewage antibiotics and therefore new low-cost technologies are needed. Adsorption is a widely used process for removal of substances, and the search for efficient, low-cost adsorbents is ongoing. In this work, termite feces treated with  $H_2SO_4$  (FT/ $H_2SO_4$ ) were used as a low-cost adsorbent for removal of norfloxacin (NOR) present in aqueous medium. Termite feces were treated with  $H_2SO_4$  at a ratio of 1:1 for 24 h, at 100 °C. The parameters contact time, initial NOR concentration, medium pH and temperature were evaluated. The optimum adsorption pH was 8.0. The pseudo-second-order model was found to best represent the kinetics of NOR adsorption. The maximum adsorption capacity, calculated from the Sips isotherm model, was 104.4 mg/g at 55 °C. The positive values of  $\Delta H^0$  (change in enthalpy) confirm the endothermic nature of the adsorption. The results show that FT/ $H_2SO_4$  is an efficient adsorbent for removal of NOR present in aqueous medium. The adsorption capacity is higher than those reported in the literature for other low-cost adsorbents.

**Key words** | antibiotics, norfloxacin, termite feces, wastewater

Tamiris Chahm  
Larissa Fátima de Souza  
Nathalia Ramos dos Santos  
Bruna Aparecida da Silva  
Clovis Antonio Rodrigues (corresponding author)  
Núcleo de Investigações Químico-Farmacêuticas (NIQFAR),  
Universidade do Vale do Itajaí (UNIVALI),  
Itajaí 88302-202, Santa Catarina,  
Brazil  
E-mail: [crodrigues@univali.br](mailto:crodrigues@univali.br)

### INTRODUCTION

Drugs are classified as emerging contaminants (EC) when found in the environment. Normally, these compounds are found in domestic, industrial and hospital wastewater (Tuc *et al.* 2017). Antibiotics are widely used to treat humans, cattle, swine, chickens and fish. Antibiotics have different half-lives when in the environment and some are very persistent. The presence of these drugs at high levels has already been reported, having a direct impact on aquatic organisms, causing changes in survival and growth (Christou *et al.* 2017; Grenni *et al.* 2018). Antibiotics are among the most important EC, as they can cause antibiotic resistance and development of super-bacteria (Christou *et al.* 2017; Grenni *et al.* 2018).

Norfloxacin (NOR), a broad-spectrum antibiotic drug that belongs to the fluoroquinolone (FQ) class of family, shows high antibacterial activity against both Gram-positive and Gram-negative bacteria through the inhibition of DNA gyrase. FQs are fourth-generation antibiotics, and more

than 60 FQs are in use after a clinical inspection certificate. FQs are the potent and broad-spectrum antimicrobial agents increasingly used as human and veterinary medicines for preventing severe or resistant bacterial infections since the late 1980s.

Norfloxacin has a good solubility in water of approximately 400 mg/L, pKa 6.22 and 8.51, and  $\log K_{ow}$  1.03 (Yang *et al.* 2012; Feng *et al.* 2018). FQs are generally excreted unmetabolized up to 70%, and have received increasing concern worldwide due to their occurrence in natural waters. FQs have shown adverse ecological impacts, mainly promoting the formation of antibiotic resistance in microbial populations.

Due to its incorrect disposal, NOR has been frequently detected in rivers and sediments (Li *et al.* 2017). Recently Feng *et al.* (2018) reported on the presence of NOR in surface water and effluents from sewage plant treatment in several regions of the world. The concentrations of NORs found in surface waters ranged from 33 to 1,150 ng/L and

effluents from 9.4 to 170 ng/L. These values varied greatly depending on the country (Riaz *et al.* 2018).

Most traditional wastewater treatment plants are not prepared for the removal of antibiotics, so treated effluent can carry a significant amount of these effluents into the environment. In this way, the removal of EC found in effluents has become the target of many researchers who work with environmental issues, especially those related to the aquatic environment (Barancheshme & Munir 2018; Turolla *et al.* 2018).

Among the various alternative effluent treatment systems, the adsorption process has been studied as the most viable alternative when the cost-benefit relation is taken into account (Gisi *et al.* 2016). The adsorption process is simple and efficient, and is usually easy to implement and operate. The adsorption process may depend on several factors, including structural and physicochemical properties of the adsorbent surface (specific surface area (SSA), functional groups active, pH<sub>Zc</sub>), and the conditions under which adsorption is carried out, such as pH, temperature, contact time, ionic strength and matrix nature (de Andrade *et al.* 2018).

A large variety of low-cost adsorbents were examined for their ability to remove EC from wastewater. Generally, the goal is to replace conventional adsorbents with low-cost activated carbons (agricultural or organic wastes). The use of these wastes as adsorbents will provide advantages in combating environmental pollution; firstly, the volume of waste can be partially reduced and, secondly, the low-cost adsorbents can reduce the wastewater pollution, at a reasonable cost. Organic residues used in the preparation of low-cost adsorbents include earthworm manure (Wang *et al.* 2017a, 2017b), silkworm feces (ElShafei *et al.* 2014), cow manure (Tzeng *et al.* 2016; Idrees *et al.* 2018), yak manure (Wang & Liu 2018) termite feces (Debrassi & Rodrigues 2011), broiler cake (Lima *et al.* 2016), swine manure (Tsai & Chen 2013; Fitzgerald *et al.* 2015), and chicken manure (Nguyen & Lee 2015; Idrees *et al.* 2018; Yu *et al.* 2018).

Several authors have successfully studied a variety of low-cost adsorbents, which are effective and readily available in large quantities for the removal of wastewater NOR. These include *Moringa oleifera* pod husk (Wuan *et al.* 2016), cauliflower roots (Qin *et al.* 2017), potato stem and natural attapulgite (Li *et al.* 2017), corn stalks, reed stalks and willow branches (Wang *et al.* 2017a, 2017b), magnetic bamboo-based activated carbon (Peng *et al.* 2018), *Calotropis gigantea* fiber (Yi *et al.* 2018), and coffee husks and rice (Paredes-Laverde *et al.* 2018).

Our objective in this study was to determine the efficiency of NOR removal by termite feces that were

activated by H<sub>2</sub>SO<sub>4</sub>, designated FT/H<sub>2</sub>SO<sub>4</sub>. The functional groups of the adsorbent were characterized by Fourier transform infrared (FTIR) spectroscopy, point of zero charge (pH<sub>pzc</sub>), SSA and Boehm titration. The effects of pH on NOR adsorption on FT/H<sub>2</sub>SO<sub>4</sub> were evaluated by kinetic and isothermal models to address the dominant driving force of NOR adsorption on FT/H<sub>2</sub>SO<sub>4</sub>. The thermodynamic parameters, and the interaction mechanism between the FT/H<sub>2</sub>SO<sub>4</sub> and NOR, were also evaluated. The method was optimized using the Box-Behnken experimental design with response surface methodology (RSM).

## EXPERIMENTAL

### Material

#### Adsorbent preparation

The termite feces were collected in the biopolymer laboratory, washed with distilled water, and mixed with concentrated H<sub>2</sub>SO<sub>4</sub> at a 1:1 (w/w) ratio. They were then kept in a greenhouse for 24 h at 100 °C. The residue was washed with distilled water until complete removal of H<sub>2</sub>SO<sub>4</sub>. The solid was oven dried, milled, and sieved and the fraction collected in a 180 mesh. This fraction was used in the experiments. The solid was designated FT/H<sub>2</sub>SO<sub>4</sub>.

#### Characterization of FT/H<sub>2</sub>SO<sub>4</sub>

Morphological analysis of the particles was performed by scanning electron microscopy (SEM). The samples were previously fixed on double-sided tape and covered with colloidal gold. The scanning electron micrographs were obtained using a Philips XL-30 scanning electron microscope. The characterization of adsorbents by FTIR spectroscopy and thermogravimetric analysis (TGA) are described in detail in the Supplementary Material (available with the online version of this paper).

The pH<sub>pzc</sub> for the FT/H<sub>2</sub>SO<sub>4</sub> was investigated by referring to the literature (Supplementary Material) (Sarma & Mahiuddin 2014). The pH<sub>pzc</sub> of the adsorbents was determined from the plot of pH<sub>final</sub> - pH<sub>initial</sub> versus pH<sub>initial</sub> of adsorbent suspensions. The SSA was determined by adsorption of methylene blue (MB) method (Yukselen & Kaya 2008). The functional groups on the surface of FT/H<sub>2</sub>SO<sub>4</sub> were determined by the Boehm method. The amount of groups on the surface of the adsorbent was analyzed as follows: NaHCO<sub>3</sub> (carboxylic groups), Na<sub>2</sub>CO<sub>3</sub> (carboxylic

groups and lactones), NaOH (carboxylic groups, lactones and phenolic groups) and HCl (basic sites) (ElShafei *et al.* 2014).

## Norfloxacin adsorption

### Effect of pH

FT/H<sub>2</sub>SO<sub>4</sub>, 25 mg, was added to an aqueous solution of NOR (100 mg/L, 20 mL, pH 4.0–12.0). The pH of the solution was adjusted with aqueous solutions of HCl or NaOH. The suspension was shaken for 24 h at 25 °C. The sample was centrifuged and the filtrate analyzed with a spectrophotometer. The concentrations of NOR were analyzed by absorbance measurements using a Jasco V-630 UV/Vis spectrophotometer, at a wavelength of 280 nm. The experiments were carried out in triplicate. The NOR adsorption capacity,  $q_e$  (mg/g), was calculated by the equation:

$$q_e = \frac{(C_0 - C_e) \times V}{M} \quad (1)$$

where  $C_0$  (mg/L) and  $C_e$  (mg/L) are the initial and equilibrium concentrations of NOR, respectively,  $V$  (L) is the volume of solution, and  $M$  (g) is the dry mass of adsorbents,

### Adsorption isotherm

Batch adsorption experiments were conducted in 125 mL Erlenmeyer flasks containing 25 mg of FT/H<sub>2</sub>SO<sub>4</sub> and 20 mL of NOR solutions with different initial concentrations (20, 35, 50, 75, 100 and 120 mg/L). The flasks were shaken for 2 h in a thermostated water bath shaker at different temperatures (25, 35, 45 and 55 °C). The experiments were carried out in triplicate. The sample was filtered using a syringe filter and the filtrate was analyzed with a spectrophotometer. The equilibrium data were analyzed using the Langmuir (S3), Freundlich (S4) and Sips (S5) isotherms, and the characteristic parameters for each isotherm were determined.

### Kinetic studies

Batch adsorption experiments were conducted in 125 mL Erlenmeyer flasks containing 25 mg of FT/H<sub>2</sub>SO<sub>4</sub> and 20 mL of NOR (50 mg/L) at 25, 40, 55 and 70 °C. The flasks were shaken at predetermined time intervals (5, 30, 45, 60, 90, 120 and 150 min). The experiments were carried out in triplicate. Aqueous samples were taken from the solution and then filtered with a syringe filter. The NOR concentration of the filtrate was analyzed with a spectrophotometer. The

kinetic data were analyzed using the pseudo-first-order and pseudo-second-order model, and the characteristic parameters for each model were determined.

The suitability, accuracy and precision of the isotherm and kinetics models were tested by the chi-squared ( $\chi^2$ ) and residual sum of squares (RSS) represented below:

$$\chi^2 = \sum_{i=1}^n \frac{(q_e - q_m)^2}{q_m} \quad (2)$$

$$\text{RSS} = \sum_{i=1}^n (q_e - q_m)_i^2 \quad (3)$$

where,  $q_e$  and  $q_m$  are the adsorption capacity obtained experimentally and determined by the isotherm adsorption model, respectively.

### Box–Behnken statistical experimental design

Factorial design is useful for studying the joint effect of different factors on a response. The Box–Behnken design consisting of three factors: temperature, pH and initial NOR concentration, at three levels was chosen based on the adsorption capacity of NOR by FT/H<sub>2</sub>SO<sub>4</sub>. The design was composed of three levels: –1 for low level, +1 for high level and 0 for the center point, and a total of 15 runs were carried out to optimize the level. The amount of adsorbent (25 mg) and the volume of the solution (20 mL) were kept constant for the experiments (15 runs).

The selected variables were temperature (A), pH (B) and NOR concentration (C). The complete design consisted of 15 experimental points, as shown in Table S1 (available online). The NOR adsorption capacity was selected as the response to the combination of independent variables, which is adjusted by a second-order polynomial model, as follows:

$$Q_e = \beta_0 + \beta_1 x_A + \beta_2 x_B + \beta_3 x_C + \beta_4 x_A^2 + \beta_5 x_B^2 + \beta_6 x_C^2 + \beta_7 x_A x_B + \beta_8 x_A x_C + \beta_9 x_B x_C \quad (4)$$

where  $\beta_0$  is the global mean representing the linear and quadratic regression coefficients related to the interactions, and  $A$ ,  $B$  and  $C$  represent the temperature, pH and initial concentration, respectively.

The analysis of variance (ANOVA), the coefficient of determination  $R^2$ , probability  $P$ -value (with 95% confidence level) and Fisher's test were used to evaluate the statistical significance. All the statistical analyses, 3D surface plots and model fitting were carried out using the statistical software package Statistica 7.0.

## RESULTS

### Characterization

As shown in Figure 1(a), the surface of treated termite feces was homogeneous, smooth, and flat. After activation (FT/H<sub>2</sub>SO<sub>4</sub>), the surface was rough and porous (Figure 1(b)) due to the dehydrating action of activating agent, which leads to the development of porosity. The particle size distribution of the activated carbon obtained in this manner was determined as  $28.7 \pm 9.6 \mu\text{m}$ , Figure 1(c).

The  $\text{pH}_{\text{pzc}}$  of FT/H<sub>2</sub>SO<sub>4</sub>, Figure 1(d), was found to be approximately pH 1.7. Therefore, for pH values above 1.7, there was a predominant negatively charged surface of FT/H<sub>2</sub>SO<sub>4</sub>. At lower pH values, the surface charge may be mainly positively charged.

According to the Boehm method (ElShafei *et al.* 2014), the functional groups at the surface of the FT/H<sub>2</sub>SO<sub>4</sub> were

phenolic 61.1 mg/g, lactonic 24.5 mg/g, and carboxylic 14.8 mg/g. The SSA determined by the MB adsorption method of FT/H<sub>2</sub>SO<sub>4</sub>, was found to be 81.3 m<sup>2</sup>/g. This SSA is large when compared to lignocellulosic walnut carbon 32.4 m<sup>2</sup>/g (Hajati *et al.* 2016), oil fly ash 63 m<sup>2</sup>/g (Labaran & Vohra 2016), eucalyptus saw dust modified with acid 0.69–1.54 m<sup>2</sup>/g (Sun *et al.* 2015), mango leaf powder 4.92 g/m<sup>2</sup> (Uddin *et al.* 2017) and other recently used biosorbents. The characterization through FTIR and thermal analysis of the FT/H<sub>2</sub>SO<sub>4</sub> are detailed in the Supplementary Material (available with the online version of this paper).

### Effect of pH

The influence of pH values ranging from 4 to 12.0 on the adsorption of NOR on FT/H<sub>2</sub>SO<sub>4</sub> was investigated, using an initial NOR concentration of 100 mg/L and a shaking time of 24 h at 25 °C (Figure 2(a)). More than 83% of

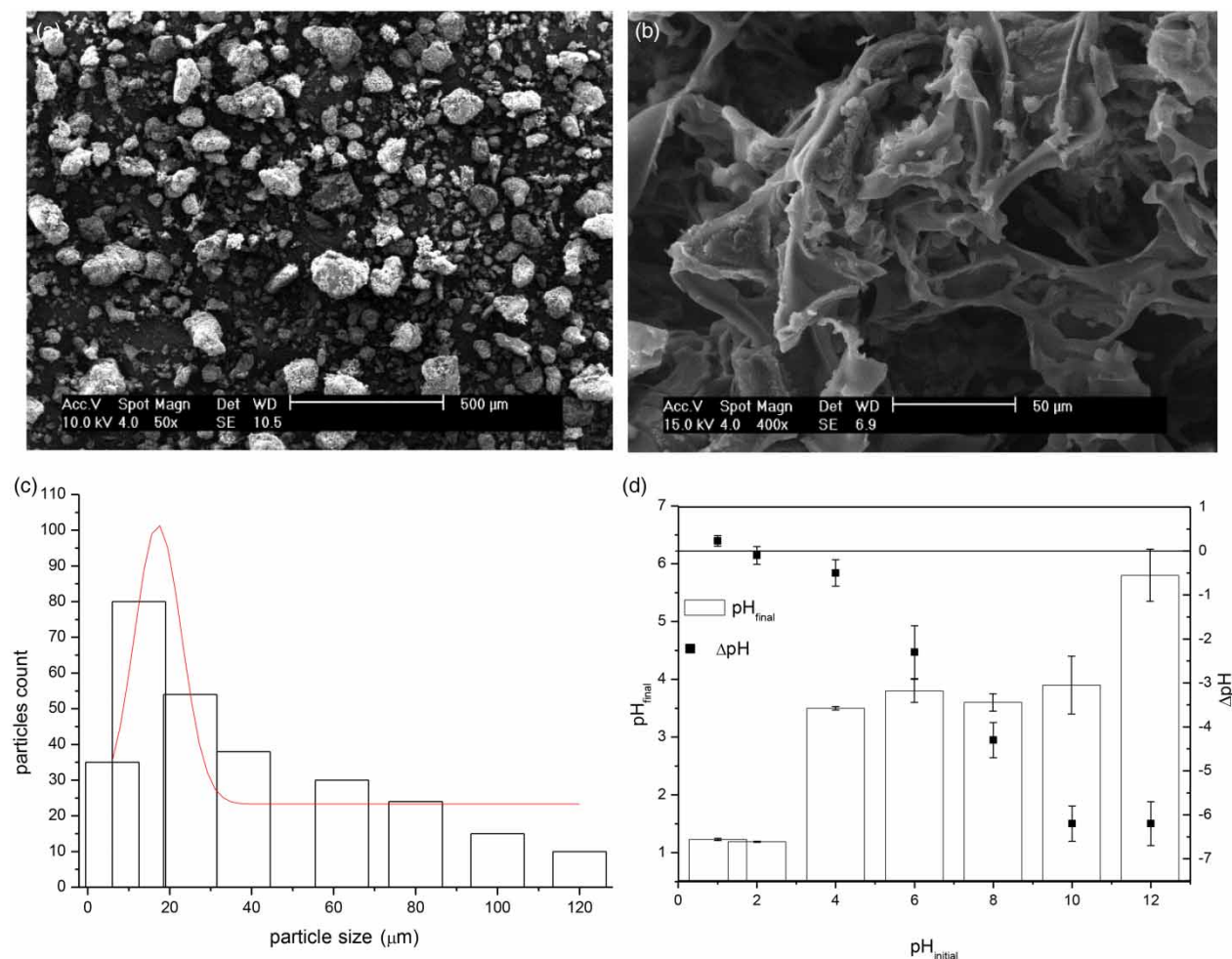


**Figure 1** | SEM image of waste of termite feces before H<sub>2</sub>SO<sub>4</sub> treatment (a) and after treatment (b), particle size distribution (c) and point of zero charge for FT/H<sub>2</sub>SO<sub>4</sub> adsorbent (d).



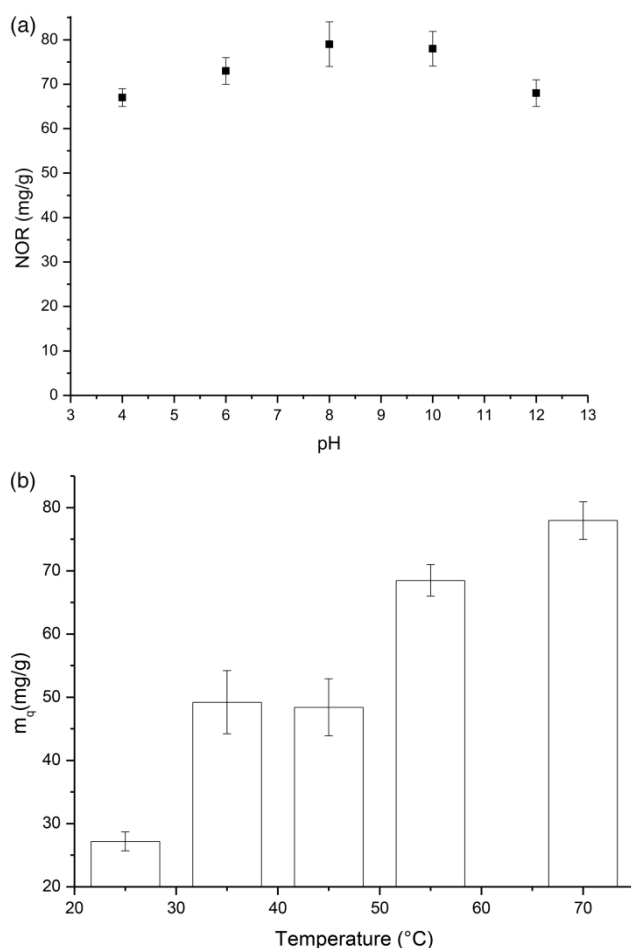


**Figure 2** | Effect of pH (a) and temperature (b) on the adsorption of the NOR onto FT/H<sub>2</sub>SO<sub>4</sub>.

NOR was removed from aqueous solution by FT/H<sub>2</sub>SO<sub>4</sub>, at a wide range of pH values, indicating that FT/H<sub>2</sub>SO<sub>4</sub> had a wide pH range of application and a high NOR removal rate. The pH 8 had the highest NOR uptake (78.9 mg/g), which corresponds to the removal of 98% of the drug initially present in the solution.

The results showed that there was little difference between the effect of different pH values of the initial solution on the adsorption of NOR onto FT/H<sub>2</sub>SO<sub>4</sub>, due to the buffer effect, shown in the study of pH<sub>pzc</sub> (Figure 1(d)). NOR is mainly in the form of a negative charge under experiment conditions (initial pH of 4.0–12.0), in which differences in electrostatic interactions between FT/H<sub>2</sub>SO<sub>4</sub> and NOR could be less significant. Similar observations were obtained by Li *et al.* (2017) and Qin *et al.* (2017).

It is known that the drug molecules are mainly adsorbed by the adsorbent via electrostatic interaction, hydrophobic–hydrophobic interaction and hydrogen bonding, and the pH

affects mainly the electrostatic interaction. NOR has two proton-sensing sites (piperazinyl and carboxyl groups) with pKa values of 6.22 and 8.51, respectively. Thus, NOR can exist in cationic form NOR<sup>+</sup>, zwitterionic and neutral form NOR<sup>±</sup>/NOR<sup>0</sup>, or anionic form NOR<sup>-</sup>, depending on the pH of the solution. At pH 4.0 approximately 100% of NOR is in cationic form, at pH 7.0 around 88.7% is in the neutral form (zwitterion), and at pH 12 100% of NOR is in anionic form (Souza *et al.* 2018).

The adsorption process of NOR in FT/H<sub>2</sub>SO<sub>4</sub> can be explained by different mechanisms. NOR has an aromatic part and functional groups which are suitable for hydrogen bonding. A dispersive force has been introduced between the free electron of NOR and the delocalized electron in the oxidized carbons ( $\pi$ - $\pi$  interaction) (Kyzas & Deliyanni 2015; Wang *et al.* 2017a, 2017b). Hydrogen bonding and electrostatic attraction through the carboxylic groups and protonated amine of NOR, respectively, seem to play significant roles in the adsorption onto the surface of carbonaceous-like adsorbents. The presence of a higher number of phenolic groups (61.1 mg/g) favors the interactions of hydrogen bonds between NOR and FT/H<sub>2</sub>SO<sub>4</sub> (Paredes-Laverde *et al.* 2018). Electron donor–acceptor interaction is one of the main driving forces in the adsorption of organic chemical molecules with benzene rings onto carbonaceous material. The binding of fluorine groups to benzene rings act as  $\pi$ -electron-acceptors due to the powerful electron withdrawing ability of N and F (Rostamian & Behnejad 2017). The hydroxyl groups present on the surface of the adsorbent (phenolic groups) can act as an electron donor.

Therefore, the  $\pi$ - $\pi$  interaction, electron donor–acceptor interaction and hydrogen bonding may be one of the main mechanisms for NOR adsorption onto FT/H<sub>2</sub>SO<sub>4</sub>.

### Effect of temperature

The effect of temperature on the adsorption rate of NOR onto FT/H<sub>2</sub>SO<sub>4</sub> was investigated at temperatures of 25–55 °C using 25 mg of FT/H<sub>2</sub>SO<sub>4</sub> (Figure 2(b)). The results show that the adsorption capacity of NOR increased proportionally to temperature, indicating that the process is endothermic. The increase in adsorption capacity was attributed to the increase in pore size and to the activation of the adsorbent surface with increased temperature. In addition, increasing the temperature is known to increase the rate of diffusion of the adsorbate molecules across the external boundary layer and in the internal pores of the adsorbent particles. Similar effects of temperature were observed by other researchers in the removal of NOR, although using

different adsorbents, such as cauliflower roots (Qin *et al.* 2017), potato peel (Kyzas & Deliyanni 2015) and potato stem (Li *et al.* 2017).

### Adsorption kinetics

The amount of NOR removed as a function of time was studied, with an initial 100 mg/L concentration of NOR and an FT/H<sub>2</sub>SO<sub>4</sub> dosage of 25 mg at 25, 40 and 55 °C. Adsorption of NOR by adsorbent occurs very rapidly and is dependent on temperature. Figure 3 shows that increasing the temperature accelerated the sorption rate of NOR and reduced the time to reach equilibrium. When the temperature was increased from 25 to 55 °C, the time needed for NOR adsorption to reach apparent equilibrium was reduced from 120 min to 60 min. There was a faster rate of adsorption at the initial stage, followed by a subsequent decrease. This may be due to the availability of a complete active bare surface. After saturating the exterior surface, NOR molecules enter the interior surface of the adsorbents, which is a relatively slow process.

The pseudo-first-order (Table S2 Equation (S1)) and pseudo-second-order (Table S2 Equation (S2)) kinetic models (available online) were used to obtain the sorption kinetics of NOR onto FT/H<sub>2</sub>SO<sub>4</sub>. The experimental data were then fitted to the pseudo-second-order equation (Figure 3 and Table 1). The kinetic data best fit the pseudo-second-order kinetic model, with a high correlation coefficient ( $R^2 > 0.97375$ ) as compared to the pseudo-first-order equation, and calculated lower values of  $\chi^2$  and RSS, and experimental  $q_e$  values (33.5, 41.4 and 43.8 mg/g) that

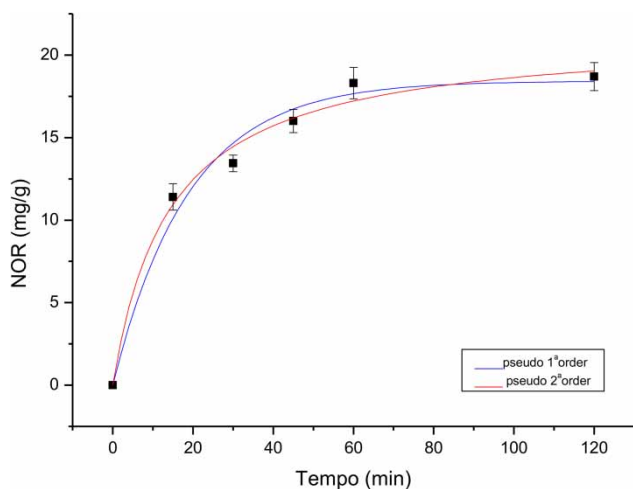


**Figure 3** | (a) Pseudo-first-order kinetics and (b) pseudo-second-order kinetics model for adsorption of the NOR onto FT/H<sub>2</sub>SO<sub>4</sub>; 20 mL of NOR solution with a concentration of 3.5 mg/L; T = 25 °C; amount of adsorbent 0.025 g.

**Table 1** | Kinetics parameters for adsorption of NOR onto FT/H<sub>2</sub>SO<sub>4</sub>

#### Pseudo-first-order

Temperature (°C)	$q_{ec}$ (mg/g)	$K_1$ (1/min)	$R^2$	$\chi^2$	RSS
25	29.3	$4.1 \times 10^{-2}$	0.9909	1.19	5.96
40	37.5	$4.7 \times 10^{-2}$	0.9504	9.75	58.56
55	36.6	$7.7 \times 10^{-2}$	0.9643	9.21	36.87

#### Pseudo-second-order

Temperature (°C)	$q_{ec}$ (mg/g)	$K_2$ (g/mg min)	$R^2$	$\chi^2$	RSS
25	33.4	$1.8 \times 10^{-3}$	0.9941	0.77	3.85
40	42.8	$1.5 \times 10^{-3}$	0.9737	5.17	31.04
55	42.1	$2.5 \times 10^{-3}$	0.9809	4.94	19.76

were close to the calculated  $q_e$  values at each temperature tested (25, 40 and 55 °C) respectively.

Therefore, the fit of the data in the model and the kinetic parameters suggests that the pseudo-second-order kinetic model was followed in the adsorption of NOR onto FT/H<sub>2</sub>SO<sub>4</sub>. This result also indicates that chemisorption may be the rate limiting step of the adsorption process, where electron sharing occurs between NOR and FT/H<sub>2</sub>SO<sub>4</sub> (Pouretedal & Sadegh 2014).

### Isotherm adsorption

Adsorption capacity is a function of the initial NOR concentration, and is therefore a very important parameter in the adsorption process. As shown in Figure 4, higher initial

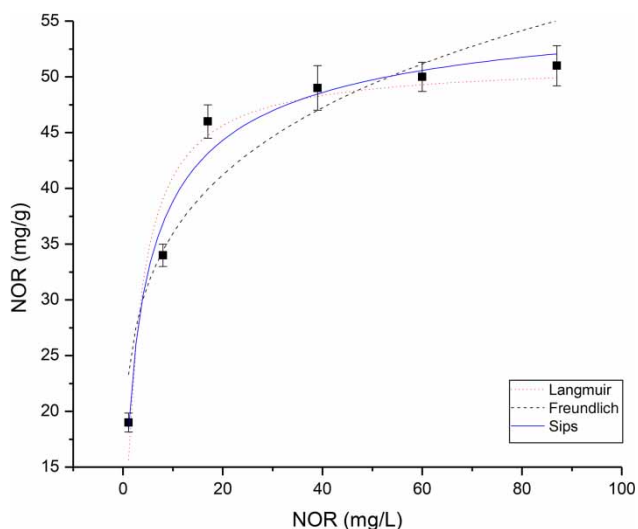


**Figure 4** | Langmuir, Freundlich and Sips isotherm model for adsorption of NOR onto FT/H<sub>2</sub>SO<sub>4</sub>; pH 7.5, T = 25 °C, amount of adsorbent 0.025 g.

concentrations of NOR resulted in increased adsorption capacity. This phenomenon may be explained by the fact that the active sites present on the surface of the adsorbents are limited in number, so that they become saturated at a certain concentration. The transport of a component from a region with a higher concentration to a region of lower concentration is referred to as a mass transfer process. This difference in concentrations is responsible for the occurrence of mass transfer; therefore the concentration gradient is the driving force. The increase in initial concentration of NOR increases the adsorption capacity. This result is in agreement with previous studies by other researchers (Sadaf & Bhatti 2014).

The results were also fitted to Langmuir (Table S3 Equation (S3)), Freundlich (Table S3 Equation (S4)) and Sips (Table S3 Equation (S5)) adsorption isotherms in non-linear form (available online). The calculated parameter of the corresponding  $R^2$ ,  $\chi^2$  and RSS values at different temperature are shown in Table 2. It is clear that the NOR adsorption process was well described by the Sips isotherm model, exhibiting the highest  $R^2$  (0.9272–0.9967), and lowest  $\chi^2$  (3.5–25.9) and RSS (0.40–77.7) that best fit the experimental data. The maximum biosorption capacity ( $q_m$ ) increased from 30.2 to 104.4 mg/g when the temperature was increased from 25 to 55 °C, suggesting that the adsorption was an endothermic process.

**Table 2** | Isotherm parameters for adsorption of NOR onto FT/H<sub>2</sub>SO<sub>4</sub>

Langmuir						
	$q_m$ (mg/g)	$K_L$ (L/g)	RSS	$\chi^2$	$R^2$	
25 °C	34.2	0.0680	2.8	1.4	0.9836	
35 °C	51.4	0.397	40.4	13.5	0.9434	
45 °C	58.8	0.222	81.9	20.4	0.9233	
55 °C	94.5	0.215	23.8	5.9	0.9927	
Freundlich						
	$K_F$ (L/g)	$C$	RSS	$\chi^2$	$R^2$	
25 °C	7.07	0.322	12.9	6.4	0.9255	
35 °C	22.8	0.196	75.9	25.3	0.8938	
45 °C	19.2	0.260	98.8	24.7	0.9075	
55 °C	26.5	0.337	149.3	37.3	0.9544	
Sips						
	$q_m$ (mg/g)	$K_S$ (L/g)	$c$	RSS	$\chi^2$	$R^2$
25 °C	30.2	0.0226	1.5	0.40	6.4	0.9976
35 °C	58.1	0.431	0.66	18.4	9.2	0.9742
45 °C	64.9	0.256	0.74	77.7	25.9	0.9272
55 °C	104.4	0.225	0.82	10.6	3.5	0.9967

**Table 3** | Comparison of different adsorbents for the adsorption of norfloxacin

Adsorbent	NOR adsorption (mg/g); (adsorption condition)	Reference
Potato stem biochar	2.6 (pH 2.9, 25 °C)	Li et al. (2017)
<i>Moringa oleifera</i> pod husks (ammonium treated)	1.5 (pH 5.0, 25 °C)	Wuan et al. (2016)
<i>Moringa oleifera</i> pod husks (carbonized)	2.0 (pH 5.0, 25 °C)	Wuan et al. (2016)
Biochar roots of cauliflowers	29.5 (pH 6.5, 25 °C)	Qin et al. (2017)
Biochar straw	349 (pH 6.9 25 °C)	Yan et al. (2017)
Rice ( <i>Oryza sativa</i> ) husk wastes	20.12 (pH 6.2, 25 °C)	Paredes-Laverdes et al. (2018)
Coffee ( <i>Coffea arabica</i> ) husk wastes	33.56 (pH 6.2, 25 °C)	Paredes-Laverdes et al. (2018)
FT/H <sub>2</sub> SO <sub>4</sub>	104 (pH 6.2, 55 °C)	In this work

The adsorption of NOR on different adsorbents reported in the literature are presented in Table 3. The  $q_m$  of this study was found to be comparable with those of other adsorbents. The results indicate that FT/H<sub>2</sub>SO<sub>4</sub> has high potential for use in the treatment of drug-contaminated wastewater.

### Thermodynamic parameters

The temperature influences the adsorption equilibrium, and its variations produce an increase in solubility of the molecules (if in liquid phase), and their diffusion within the pores of the adsorbent materials (Anastopoulos & Kyzas 2016). To determine the effects of temperature on NOR adsorption, adsorption experiments were conducted at 25–55 °C. The thermodynamic parameters were determined using Table S4, Equations (S6)–(S8), and Figure S3 (Supplementary Material, available online).

Table 4 shows the thermodynamic parameters determined for the adsorption system. The negative value of  $\Delta G^0$  at 55 °C indicates the spontaneous nature of NOR

**Table 4** | Thermodynamic parameters

$\Delta H^0$ (kJ/mol K)	$\Delta S^0$ (J/mol)	$\Delta G^0$ (kJ/mol)	$R^2$
62.62	198.7	(298) <sup>a</sup> 2.8	–0.9612
		(308) 1.38	
		(318) 0.185	
		(328) – 3.54	

<sup>a</sup>Numbers in brackets refer to temperature (K).

adsorption at 55 °C. In addition, a decrease in  $\Delta G^0$  values with an increase in temperature indicates that the adsorption is more spontaneous at higher temperatures. The  $\Delta H^0$  values were found to be positive (62.6 kJ/mol K), which indicated the endothermic nature. Positive values were found for  $\Delta S^0$  (198.7 J/mol K), which reflects the increased randomness at the solid–liquid interface during the sorption and indicates an affinity of FT/H<sub>2</sub>SO<sub>4</sub> for NOR.

## RESPONSE SURFACE METHODOLOGY

The RSM was used to determine the importance of the pH, NOR concentration and temperature on the drug adsorption. Considering the Box–Behnken design, three levels were chosen for each of three independent variables, as indicated in Table S5 (available with the online version of this paper), using the three levels of  $-1$ ,  $0$ , and  $+1$  and equally spaced intervals. Significant and insignificant terms were determined, and then the predictive model was obtained. The removal of NOR by FT/H<sub>2</sub>SO<sub>4</sub> in terms of the significant factors is given in Equation (5)

$$Y = 24.62 + 15.70A + 4.99A^2 + 13.98B + 9.62C - 10.65C^2 \quad (5)$$

Based on the coefficients in Equation (5), it can be concluded that by increasing the temperature (both linear and quadratic), pH (linear term) and NOR concentration (linear term), NOR adsorption rises; whereas, by increasing pH (quadratic term), NOR adsorption decreases. The main effects and the interaction effects of each factor with a  $P$ -value  $<0.05$  are considered potentially significant. The temperature (A) had the greatest effect on removal efficiency, followed by pH (B), NOR concentration (C<sup>2</sup>), NOR concentration (C), and temperature (A<sup>2</sup>). On the other hand, pH (B<sup>2</sup>) has little effect on the adsorption of NOR.

According to the ANOVA analysis shown in Table S6 (available online), the linear term temperature had the greatest effect on NOR adsorption, with an  $F$ -value of 53.70, followed by linear term pH, quadratic term NOR concentration, linear term NOR concentration and quadratic term temperature, with  $F$ -values of 49.78, 42.65, 18.62 and 9.37, respectively.

The SS was used to calculate the percentage contribution of each model term, since these quantities are predominant in the biosorption process, as the value of SS intensifies the significance of the corresponding source in the process. As shown in Table S6, the temperature of the

solution showed the highest level of significance with a contribution of 24.08% (linear term), followed by pH with 22.31% (quadratic terms) and NOR concentration with a contribution of 19.14% (linear term) as compared to other components.

The goodness of the model in the present study resulted in the values of  $R^2$  and adjusted  $R^2$  values of 0.9641 and 0.9372 and is in reasonable agreement with the experimental results, suggesting that 96% of total variation for NOR adsorption can be revealed by the model and only 4% is left with residual variability.

The relationship between predicted and observed values of response regarding adsorption capacity for NOR by FT/H<sub>2</sub>SO<sub>4</sub> is shown in Figure S4 (available online), which shows that the maximum number of predicted responses and their residuals for each run were reasonably close to the diagonal line, suggesting that the model is adequate and statistically valid.

The Pareto chart of standardized effects shows the influence of each individual factor (linear and quadratic) investigated on the analytical response, as well as their interactions. The positive and negative effects of the variables/parameters on the analytical response (NOR adsorption efficiency) are represented by horizontal bars. It should be noted that the length of the bar is proportional to the magnitude of statistically significant effects of each individual factor with respect to response. It can be seen from Figure S5 that sample temperature (linear term) has the significant influence on NOR adsorption, followed by pH (linear term) and NOR concentration (quadratic term).

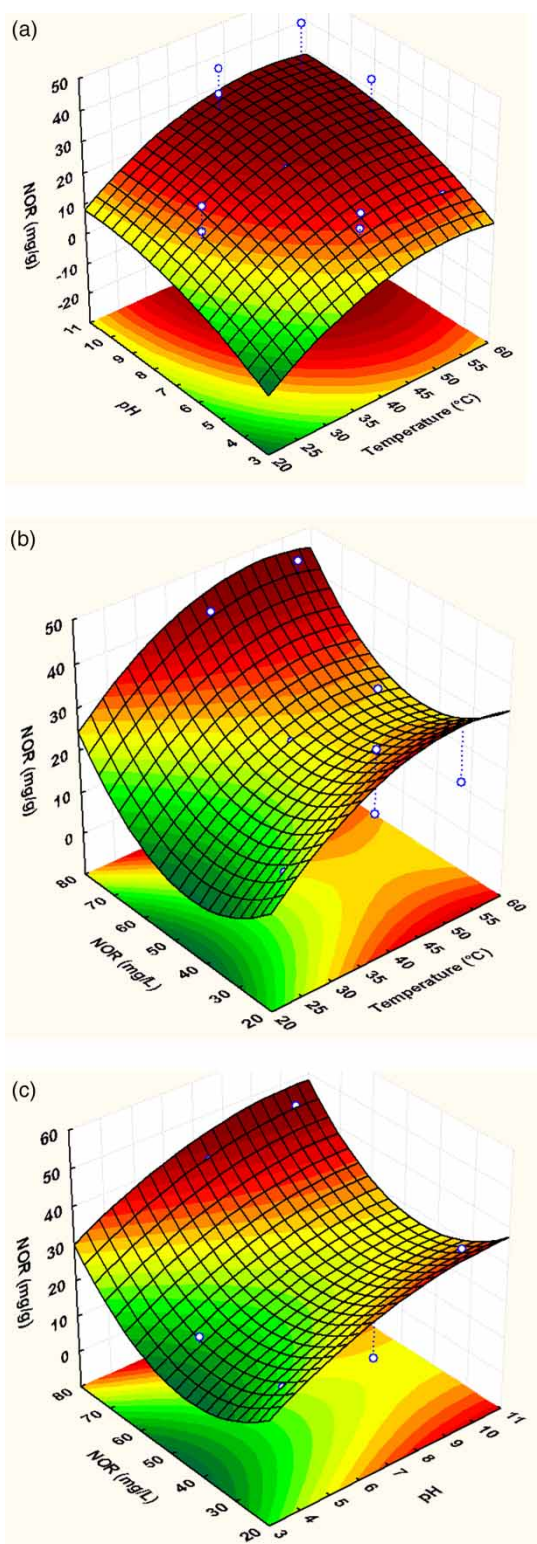
The effect of interaction between temperature and pH on NOR adsorption can be observed by 3D response surface plots generated by RSM, as shown in Figure 5.

Figure 5(a) indicates the simultaneous effect of pH and temperature on NOR adsorption efficiency for FT/H<sub>2</sub>SO<sub>4</sub> (at a constant NOR concentration of 50 mg/L). The NOR adsorption efficiency increased with an increase in pH from 2 to 11 and temperature (25–55 °C), and the maximum efficiency was obtained with pH 11 and 60 °C (43 mg/g).

Figure 5(b) shows the effect of NOR concentration and temperature (at constant pH 7.0): the adsorption efficiency increases with an increase in NOR concentration and temperature, and maximum adsorption was obtained with a temperature of 55 °C and NOR concentration of 80 mg/L (52 mg/g).

The fitted surface plot of NOR adsorption versus the combined effect of initial NOR concentration and pH solution (at a constant temperature of 40 °C) is also shown in Figure 5(c). It can be seen that the NOR adsorption





**Figure 5** | Surface response of NOR amount adsorbed (mg/g): pH x temperature (a), initial NOR concentration x temperature (b) and initial NOR concentration x pH (c).

efficiency increased with an increase in pH and NOR concentration, and maximum efficiency was obtained with

**Table 5** | Analysis of cost of preparation of FT/H<sub>2</sub>SO<sub>4</sub>

Reagent/Energy	Unit cost in US\$	Amount per kg FT/H <sub>2</sub> SO <sub>4</sub>	Net price in US\$ per kg
H <sub>2</sub> SO <sub>4</sub> (Sigma-Aldrich)	25.94 per kg	0.5 kg	12.97
Activation energy consumed	0.14 per kWh	9.6 kWh (110 °C for 24 h)	1.34
Water consumed (washing)	1.07 per m <sup>3</sup>	0.05 m <sup>3</sup>	0.054
Net cost			14.33
Other cost (10% net cost)			1.143
Total cost			15.47
Commercial activated carbon (Sigma-Aldrich)			105.60

pH 11 and 80 °C (53 mg/g). The effect of NOR concentration is so decisive that reducing or increasing the pH had a comparatively negligible effect on adsorption.

Cost analysis is an important parameter in the selection of adsorbent for the removal of drugs from wastewater. Currently, commercial activated carbon is used as adsorbent in the treatment process, but it is very expensive. There is an urgent need for a low-cost adsorbent that is as effective as commercial activated carbon, and is readily available in nature. This work is based on H<sub>2</sub>SO<sub>4</sub> impregnated termite feces. Details of the cost analysis are shown in Table 5.

## CONCLUSION

The present study showed that FT/H<sub>2</sub>SO<sub>4</sub> a low-cost waste. It was demonstrated that this adsorbent can be successfully used for the adsorption of NOR from water solution, and that its maximum adsorption capacity is comparable to that of other biosorbents reported in the literature. Based on the experiments, we observed that adsorption depends on the initial concentration, pH and temperature. The kinetics of NOR adsorption on FT/H<sub>2</sub>SO<sub>4</sub> was found to follow a pseudo-second-order rate equation. The thermodynamic parameters showed that the process is spontaneous, and is endothermic. The Sips model best fit the experimental results ( $R^2 > 0.983$ ). The maximum adsorption efficiency of NOR on FT/H<sub>2</sub>SO<sub>4</sub> was found to be 104.4 mg/g. The

study of factorial design showed three important effects: NOR concentration (quadratic term) pH (linear term) and temperature.

## ACKNOWLEDGEMENTS

This study was financed in part by the Coordenação de Aperfeiçoamento de Pessoal de Nível Superior – Brasil (CAPES) – Finance Code 001.

## REFERENCES

- Anastopoulos, I. & Kyzas, G. Z. 2016 Are the thermodynamic parameters correctly estimated in liquid-phase adsorption phenomena? *Journal of Molecular Liquids* **218**, 174–185.
- Barancheshme, F. & Munir, M. 2018 Strategies to combat antibiotic resistance in the wastewater treatment plants, *Frontiers in Microbiology*. <https://doi.org/10.3389/fmicb.2017.02603>
- Christou, A., Agüera, A., Bayona, J. M., Cytryn, E., Fotopoulos, V., Lambropoulou, D., Manaia, C. M., Michael, C., Revitt, M., Schroder, P. & Fatta-Kassinos, D. 2017 The potential implications of reclaimed wastewater reuse for irrigation on the agricultural environment: the knowns and unknowns of the fate of antibiotics and antibiotic resistant bacteria and resistance genes – a review. *Water Research* **123**, 448–467.
- de Andrade, J. R., Oliveira, M. F., da Silva, M. G. C. & Vieira, M. G. A. 2018 Adsorption of pharmaceuticals from water and wastewater using nonconventional low-cost materials: a review. *Industrial Engineering Chemistry Research* **57**, 3103–3127.
- Debrassi, A. & Rodrigues, C. A. 2011 Adsorption of cationic dyes from aqueous solution by termite feces, a non-conventional adsorbent. *Clean – Soil, Air, Water* **39**, 549–556.
- ElShafei, G. M. S., ElSherbiny, I. M. A., Darwish, A. S. & Philip, C. A. 2014 Silkworms' feces-based activated carbons as cheap adsorbents for removal of cadmium and methylene blue from aqueous solutions. *Chemical Engineering Research and Design* **92**, 461–470.
- Feng, M., Wang, Z., Dionysiou, D. D. & Sharma, V. K. 2018 Metal-mediated oxidation of fluoroquinolone antibiotics in water: a review on kinetics, transformation products, and toxicity assessment. *Journal of Hazardous Materials* **344**, 1136–1154.
- Fitzgerald, S., Kolar, P., Classen, J., Boyette, M. & Das, L. 2015 Swine manure char as an adsorbent for mitigation of *p*-cresol. *Environmental Progress & Sustainable Energy* **34**. DOI 10.1002/ep.
- Gisi, S. D., Lofrano, G., Grassi, M. & Notarnicola, M. 2016 Characteristics and adsorption capacities of low-cost sorbents for wastewater treatment: a review. *Sustainable Materials and Technologies* **9**, 10–40.
- Grenni, P., Ancona, V. & Caracciolo, A. B. 2018 Ecological effects of antibiotics on natural ecosystems: a review. *Microchemical Journal* **136**, 25–39.
- Hajati, S., Ghaedi, M. & Mazaheri, H. 2016 Removal of methylene blue from aqueous solution by walnut carbon: optimization using response surface methodology. *Desalination and Water Treatment* **57**, 3179–3193.
- Idrees, M., Batool, S., Kalsoom, T., Yasmeen, S., Kalsoom, A., Raina, S., Zhuang, Q. & Kong, J. 2018 Animal manure-derived biochars produced via fast pyrolysis for the removal of divalent copper from aqueous media. *Journal of Environmental Management* **213**, 109–118.
- Kyzas, G. Z. & Deliyanni, E. A. 2015 Modified activated carbons from potato peels as green environmental-friendly adsorbents for the treatment of pharmaceutical effluents. *Chemical Engineering Research and Design* **97**, 135–144.
- Labaran, B. A. & Vohra, M. S. 2016 Application of activated carbon produced from phosphoric acid-based chemical activation of oil fly ash for the removal of some charged aqueous phase dyes: role of surface charge, adsorption kinetics, and modeling. *Desalination and Water Treatment* **57**, 16034–16052.
- Li, Y., Wang, Z., Xie, X., Zhu, J., Li, R. & Qin, T. 2017 Removal of Norfloxacin from aqueous solution by clay-biochar composite prepared from potato stem and natural attapulgit. *Colloids and Surfaces A: Physicochemical and Engineering Aspects* **514**, 126–136.
- Lima, I., Klasson, K. T. & Uchimiya, M. 2016 Selective release of inorganic constituents in broiler manure biochars under different post-activation treatments. *Journal of Residuals Science & Technology* **13**, 37–48.
- Nguyen, M. V. & Lee, B. K. 2015 Removal of dimethyl sulfide from aqueous solution using cost-effective modified chicken manure biochar produced from slow pyrolysis. *Sustainability* **7**, 15057–15072.
- Paredes-Laverde, M., Silva-Agredo, J. & Torres-Palma, R. A. 2018 Removal of norfloxacin in deionized, municipal water and urine using rice (*Oryza sativa*) and coffee (*Coffea arabica*) husk wastes as natural adsorbents. *Journal of Environmental Management* **213**, 98–108.
- Peng, X., Hu, F., Zhang, T., Qiu, F. & Dai, H. 2018 Amine-functionalized magnetic bamboo-based activated carbon adsorptive removal of ciprofloxacin and norfloxacin: a batch and fixed-bed column study. *Bioresource Technology* **249**, 924–934.
- Pouretedal, H. R. & Sadegh, N. 2014 Effective removal of amoxicillin, cephalixin, tetracycline and penicillin G from aqueous solutions using activated carbon nanoparticles prepared from vine wood. *Journal of Water Process Engineering* **1**, 64–73.
- Qin, T., Wang, Z., Xie, X., Xie, C., Zhu, J. & Li, Y. 2017 A novel biochar derived from cauliflower (*Brassica oleracea* L.) roots could remove norfloxacin and chlortetracycline efficiently. *Water Science and Technology* **76**, 3307–3318.
- Riaz, L., Mahmood, T., Khalid, A., Rashid, A., Siddique, M. B. A., Kamal, A. & Coyne, M. S. 2018 Fluoroquinolones (FQs) in the

- environment: a review on their abundance, sorption and toxicity in soil. *Chemosphere* **191**, 704–720.
- Rostamian, R. & Behnejad, H. 2017 A unified platform for experimental and quantum mechanical study of antibiotic removal from water. *Journal of Water Process Engineering* **17**, 207–215.
- Sadaf, S. & Bhatti, H. N. 2014 Batch and fixed bed column studies for the removal of Indosol Yellow BG dye by peanut husk. *Journal of the Taiwan Institute of Chemical Engineers* **45**, 541–553.
- Sarma, J. & Mahiuddin, S. 2014 Specific ion effect on the point of zero charge of  $\alpha$ -alumina and on the adsorption of 3,4-dihydroxybenzoic acid onto  $\alpha$ -alumina surface. *Colloids and Surfaces A: Physicochemical Engineering Aspects* **457**, 419–424.
- Souza, D. I., Dottein, E. M., Giacobbo, A., Rodrigues, M. A. S., Pinho, M. N. & Moura, B. A. 2018 Nanofiltration for the removal of norfloxacin from pharmaceutical effluent. *Journal of Environmental Chemical Engineering* **6**, 6147–6153.
- Sun, L., Chen, D., Wan, S. & Yu, Z. 2015 Performance, kinetics, and equilibrium of methylene blue adsorption on biochar derived from eucalyptus saw dust modified with citric, tartaric, and acetic acids. *Bioresource Technology* **198**, 300–308.
- Tsai, W. T. & Chen, H. R. 2013 Adsorption kinetics of herbicide paraquat in aqueous solution onto a low-cost adsorbent, swine-manure-derived biochar. *International Journal of Environmental Science and Technology* **10**, 1349–1356.
- Tuc, D. Q., Elodie, M. G., Pierre, L., Fabrice, A., Marie-Jeanne, T., Martine, B., Joelle, E. & Marc, C. 2017 Fate of antibiotics from hospital and domestic sources in a sewage network. *Science of the Total Environment* **575**, 758–766.
- Turolla, A., Cattaneo, M., Marazzi, F., Mezzanotte, V. & Antonelli, M. 2018 Antibiotic resistant bacteria in urban sewage: role of full-scale wastewater treatment plants on environmental spreading. *Chemosphere* **191**, 761–769.
- Tzeng, T. W., Liu, Y. T., Deng, Y., Hsieh, Y. C., Tan, C. C., Wang, S. L., Huang, S. T. & Tzou, Y. M. 2016 Removal of sulfamethazine antibiotics using cow manure-based carbon adsorbents. *International Journal of Environmental Science and Technology* **13**, 973–984.
- Uddin, T., Rahman, A., Rukanuzzaman & Islam, A. 2017 A potential low cost adsorbent for the removal of cationic dyes from aqueous solutions. *Applied Water Science* **7**, 2831–2842.
- Wang, Y. & Liu, R. 2018 H<sub>2</sub>O<sub>2</sub> treatment enhanced the heavy metals removal by manure biochar in aqueous solutions. *Science of the Total Environment*. **628–629**, 1139–1148.
- Wang, B., Jiang, Y. S., Li, F. Y. & Yang, D. Y. 2017a Preparation of biochar by simultaneous carbonization, magnetization and activation for norfloxacin removal in water. *Bioresource Technology* **233**, 159–165.
- Wang, Z., Shen, D., Shen, F., Wuc, C. & Xiao, R. 2017b Low cost earthworm manure-derived carbon material for the adsorption of Cu<sup>2+</sup> from aqueous solution: impact of pyrolysis temperature Bin Zhou. *Ecological Engineering* **98**, 189–195.
- Wuan, R. A., Sha'Ato, R. & Iorhen, S. 2016 Preparation, characterization, and evaluation of *Moringa oleifera* pod husk adsorbents for aqueous phase removal of norfloxacin. *Desalination and Water Treatment* **57**, 11904–11916.
- Yan, B., Niu, C. H. & Wang, J. 2017 Kinetics, electron-donor-acceptor interactions, and site energy distribution analyses of norfloxacin adsorption on pretreated barley straw. *Chemical Engineering Journal* **330**, 1211–1221.
- Yang, W., Lu, Y., Zheng, F., Xue, X., Li, N. & Liu, D. 2012 Adsorption behavior and mechanisms of norfloxacin onto porous resins and carbon nanotube. *Chemical Engineering Journal* **179**, 112–118.
- Yi, L., Liang, G., Xiao, W., Duan, W., Wang, A. & Zheng, Y. 2018 Rapid nitrogen-rich modification of *calotropis gigantea* fiber for highly efficient removal of fluoroquinolone antibiotics. *Journal of Molecular Liquids* **256**, 408–415.
- Yu, J., Zhang, X., Wang, D. & Li, P. 2018 Adsorption of methyl orange dye onto biochar adsorbent prepared from chicken manure. *Water Science and Technology*. DOI: 10.2166/wst.2018.003.
- Yukselen, Y. & Kaya, A. 2008 Suitability of the methylene blue test for surface area, cation exchange capacity and swell potential determination of clayey soils. *Engineering Geology* **102**, 38–45.

First received 23 October 2018; accepted in revised form 17 January 2019. Available online 1 February 2019